A043

Blended Acquisition with Optimized Dispersed Source Arrays

A.J. Berkhout (Delft University of Technology) & G. Blacquiere* (Delft University of Technology)

SUMMARY

Until now, blended source arrays are configured with closely spaced source units, such as broadband airgun arrays (marine) and broadband vibrator arrays (land). In the latter case the source units are equal. We refer to this concept as homogeneous blending. In this paper the blending concept is extended to inhomogeneous blending, meaning that a blended source array consists of different source units that may be far apart. We propose for these units simple narrowband sources with different central frequencies.

Introduction

In the recent literature, already an abundance of references on blended acquisition can be found. Examples are Beasley (2008), Berkhout (2008), Howe et al. (2009), and Pecholcs et al. (2010). A blended wavefield is generated by firing a multitude of sources, each source with its own code, together forming a blended source array. Unlike a traditional source array, a blended source array covers a large spatial area, illuminating each subsurface gridpoint from different angles. The goal of blending is to improve the illumination of the subsurface without (significantly) increasing the total survey time and the operational cost per km^2. In traditional seismic surveys, each source transmits the full temporal frequency band ranging over many octaves. In practice, it requires a lot of effort to successfully produce and operate wideband sources. More important, such source designs are always a compromise. E.g., a large vibrator base plate is preferred for the low frequencies, but then the vibrator would not be able to transmit high frequencies at large angles. We propose that the source units in a blended array are not chosen to be equal and they do not need to satisfy the wideband requirements. Instead, they may be narrowband designs, which are technically simpler and operationally easier to handle. The spatial sampling of each narrowband source type and, in the marine case, its deployment depth are optimized. The criterion is that the *combined* incoherent source wavefield has the required temporal and angular spectral properties in the subsurface.

Theory

Seismic data can be arranged in data matrix **P**. In the frequency domain, element $P_{ij}(z_d, z_s)$ is a complex-valued number representing one frequency component of the trace at detector position i due to source j, located at depth levels z_d and z_s respectively. The model of data matrix $\mathbf{P}(z_d,z_s)$ can be written as (Berkhout, 1982):

$$\mathbf{P}(z_d, z_s) = \mathbf{D}^-(z_d)\mathbf{X}(z_d, z_s)\mathbf{S}^+(z_s). \quad (1)$$

In detector matrix $\mathbf{D}^-$ each row represents a receiver array, generating one seismic trace. Note that acquisition matrices $\mathbf{S}^+$ and $\mathbf{D}^-$ include the interaction with the reflective surface (often referred to as the ghost effect). Similarly, the result of one *blended* experiment is given by (Berkhout, 2008):

$$\sum_k \vec{P}(z_d, z_s)\Gamma_{kj}(z_s) = \mathbf{D}^-(z_d)\mathbf{X}(z_d, z_s)\sum_k \vec{S}_k^+(z_s)\Gamma_{kj}(z_s). \quad (2)$$

Elements $\Gamma_{kj}(z_s)$ of blending vector $\vec{\Gamma}_j(z_s)$ are complex valued scalars, describing time delays or a more complex code, while the involved sources are indicated by k: $\vec{S}_k^+$ is the k^{th} column of **S**. Equation 2 can be made specific for marine data by introducing the ghost effect:

$$\sum_k \vec{P}(z_d, z_k)\Gamma_{kj}(z_k) = \mathbf{D}^-(z_d)\mathbf{X}(z_d, z_0)\sum_k \vec{S}_k^+(z_0, z_k)\Gamma_{kj}(z_k), \quad (3)$$

where each unit k of the blended source array is allowed to be at a different depth z_k and z_0 represents the level of the water surface Assuming a surface reflectivity of -1,

$$\vec{S}_k^+(z_0, z_k) = \mathbf{W}^*(z_0, z_k)\vec{S}_k^+(z_k) - \mathbf{W}(z_0, z_k)\vec{S}_k^-(z_k). \quad (4)$$

In equation 4 matrix $\mathbf{W}^*(z_0, z_k)$ equals the propagation operator, describing the propagation between depth z_k of source unit k and surface level z_0, and superscript * denotes the conjugate complex.
Let us now consider the illumination properties of a blended source array. The incident wavefield at gridpoint i at depth level z_m being illuminated by blended source array j with source units at depth level z_s (see also equation 2) is given by:

$$P_{ij}^+(z_m, z_s) = \vec{W}_i^\dagger(z_m, z_s)\sum_k \vec{S}_k^+(z_s)\Gamma_{kj}(z_s), \quad (5)$$

where superscript † denotes a row vector and $\vec{W}_i^\dagger$, being the i^{th} row of matrix **W**, describes wavefield propagation from all source points (k) at surface level z_s to subsurface gridpoint i at depth level z_m (many-to-one projection). The imaging step in migration should take the complex

spectral properties of the incident wavefield into account, meaning that cross correlation is not acceptable anymore and that the traditional imaging principle should be replaced by a minimization process (Verschuur and Berkhout, 2011). For shot record migration this means:

$$\vec{P}_j^-(z_m,z_s)-\sum_i \vec{R}_i^{\cup}(z_m,z_m)P_{ij}^+(z_m,z_s)=\text{minimum for all } j\,, \qquad (6)$$

the minimization process being carried out for all depth levels z_m. In equation 6 vector $\vec{P}_j^-(z_m,z_s)$ equals the reflected wavefields at depth level z_m and vector $\vec{R}_i^{\cup}(z_m,z_m)$ equals the i^{th} column of reflectivity matrix $\mathbf{R}^{\cup}(z_m,z_m)$ representing the angle-dependent reflection property at gridpoint i. Equation 7 confirms the importance of the temporal and spatial spectral properties of incident wavefield $P_{ij}^+(z_m,z_s)$.

Inhomogeneous Blending

For the design of blended source arrays, incident wavefield $P_{ij}^+(z_m,z_s)$ must be judged by its temporal and spatial spectral properties. From equation 2 it follows that the individual sources at surface locations k ($\vec{S}_k^+\Gamma_{kj}$) need to be optimized by considering the properties of the composite incident wavefield at subsurface locations i (P_{ij}^+). It means that the individual sources of a blended array may consist of narrowband sources with different central frequencies, as long as the sum of all arriving components satisfies the full bandwidth requirements. We refer to this concept as inhomogeneous blending. Figure 1 illustrates the principle by showing a blended shot record with five broadband source units (Figure 1a) and five narrowband source units (Figure 1b). We call this type of blended source configuration: Dispersed Source Array (DSA). Inhomogeneous blending with DSAs has a number of attractive potential advantages:

- The narrowband units of a blended array represent simple, technically optimized sources,
- Destructive interference within a source array is avoided for angle-independent source wavelets,
- Each source type has its own spatial sampling interval, allowing multi-scale acquisition grids,
- Each source element has its own depth level, allowing ghost matching in the field (marine),
- Frequency shaping becomes an option during acquisition,
- DSAs are more flexible to comply with the emerging regulation on sea life protection (marine).

All these potential advantages need be further developed and realized in the field. E.g., in marine the advantage of different source depths (z_k) may be maximized by choosing the central frequency (f_c) of each source element in the first maximum of the ghost transfer function (ghost matching): $f_c z_k = 0.25 c_w$, c_w being the water velocity. It is interesting to mention that recently the variable depth option was proposed at the detector side, showing excellent results (Soubaras, 2010). The increasing number of sources has a practical limitation from a logistics point of view. The use of simple autonomous source boats with single airguns of different sizes (marine) and simple autonomous source trucks with

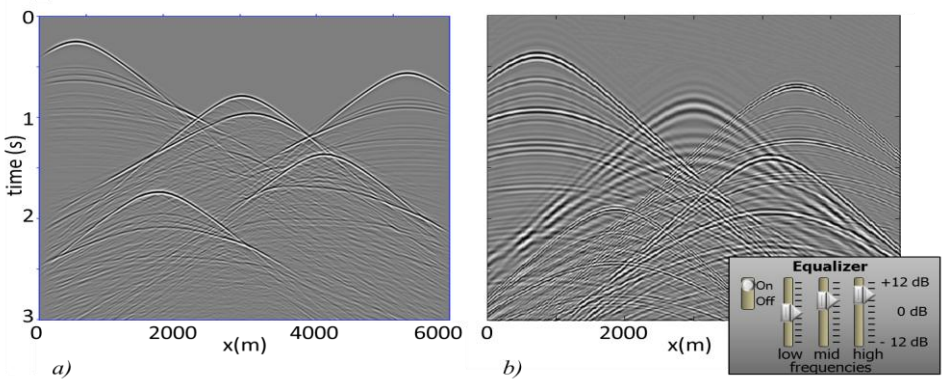

Figure 1 *In a) five broadband source units were blended whereas in b) five narrowband source units were blended: two high-frequency, two mid-frequency and one low-frequency source unit.*

single vibrators of different sizes (land) becomes a practical pro-position in DSA acquisition. It may lead to a far reaching robotization process in seismic operations.

Dispersed source array example

To illustrate the principle, a homogeneous medium is considered. Three source types are used: low- (5 Hz - 15 Hz), mid- (10 Hz - 30 Hz) and high-frequency sources (25 Hz - 75 Hz). One could think of (marine) vibrators with different central frequencies. Each of these vibrators has a relatively small bandwidth, making them technically and operationally simple with respect to broadband alternatives. Because of sampling requirements, we have chosen the numbers of low-, mid-, and high-frequency sources according to multiples of 1, 2 and 5 respectively. Note that these numbers are related to the central frequency of each of the source types. In this 2D illustration 48 sources were blended along a line of 6 km length: 6 low-, 12 mid- and 30 high-frequency sources. The blending codes were simple: time delays only. All source types were deployed at the same depth of 7.5 m. The incident wavefield ($\vec{P}_j^+$) due to this blended source configuration was computed for all gridpoints at a depth level of 1000 m (Figure 2a). Note the incoherent character of this wavefield. The different source types can be easily recognized. Although none of the sources produces the required full temporal bandwidth, the spectrum of the total incident wavefield at depth level z_m, $P_{ij}^+(z_m, z_s)$ does contain the full temporal spectrum (Figure 2c). The signal illuminating the middle gridpoint, $P_{ij}^+(z_m, z_s)$, is visualized in

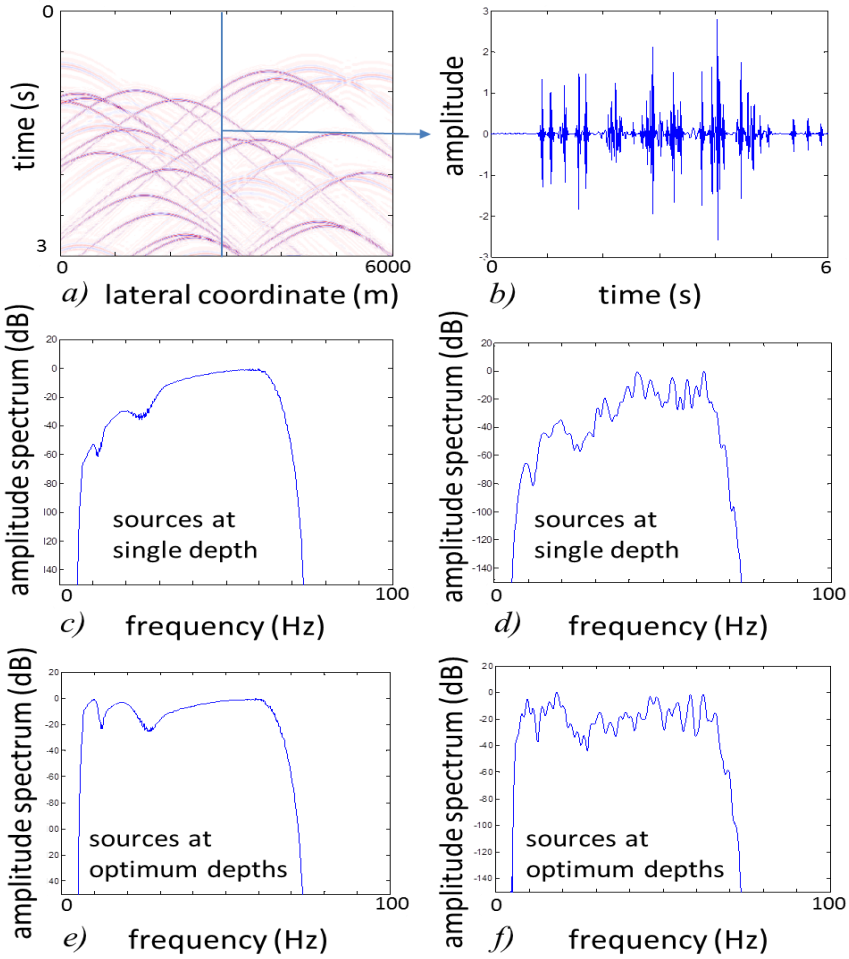

Figure 2 *a) The incident wavefield at depth level 1000 m due to 48 blended sources at the surface. The contribution of the low-, mid-, and high-frequency sources can be clearly distinguished. For clarity, only the first three seconds of data are shown. b) The middle trace of a). c) Spectrum of a). d) Spectrum of b). e) Spectrum to be compared with c) but now with optimum source depths. f) Spectrum to be compared with d) but now with optimum source depths.*

Figure 2b, showing a dispersed time series. The temporal spectrum of the windowed autocorrelation of $P_{ij}^{+}(z_m, z_0)$ is shown in Figure 2d. As expected, the full bandwidth is present because the contributions of all DSA units of the blended source array are arriving at this gridpoint. It is therefore illuminated by all temporal frequencies. Figures 2c and 2d show the well-known effect that the low frequencies are attenuated due to the surface ghost when the sources are deployed relatively shallow. In the DSA concept each source is deployed individually. Therefore, it is easy to optimize the source depth for each particular narrowband source type. As already mentioned, the optimum source depth corresponds to a quarter of its central wavelength: $z_k = 0.25 c_w / f_c$. Figures 2e and 2f show the results for the case that each source type has been deployed at its optimum depth. Notice that the low frequencies are no longer attenuated and the temporal spectrum is flat. Here, the three source types can still be recognized in the spectrum. Obviously, if desired, this effect could be reduced by having narrowband sources in more than three frequency classes.

Conclusions

In traditional seismic acquisition each source transmits the full temporal bandwidth from a single location. This makes the current seismic sources complex technical systems. Blended seismic acquisition allows the use of many more source units at many more locations for the same survey time. We propose to choose for these units narrow-band versions, with the condition that the total incident wavefield in the subsurface exhibits the required spectral properties. As a consequence, these narrow-band sources can be the result of no-compromise designs. In addition they will be less complex, more easy to operate and more effective in emission (no destructive interference within the source array).
With a multitude of narrow-band source units, being referred to as Dispersed Source Array, the blended incident wavefield at a particular subsurface gridpoint will contain the full temporal bandwidth. The incident wavefield at a subsurface gridpoint is represented by a dispersed time series, corresponding to a complex code, even if a simple source code like time delays is used. This time series contains broadband, multi-angle, multi-azimuth information. The theoretical spatial sampling requirements can be fulfilled by allowing low-frequency sources to be distributed more sparsely than high-frequency sources. In the marine situation source depths can be optimized (ghost matching).

Acknowledgement

We would like to thank the Delphi sponsors for the stimulating discussions and the financial support.

References

Beasley, C.J. [2008] A new look at marine simultaneous sources. *The Leading Edge*, **27**, 7, 914-917.

Berkhout, A.J. [2008] Changing the mindset in seismic data acquisition. *The Leading Edge*, **27**, 7, 924–938.

Blacquière, G., and Berkhout, A.J. [2010] Acquisition design for incoherent shooting. *72nd EAGE Conference & Exhibition*, Extended Abstracts, B032.

Howe, D., Foster, M., Allen, T., Jack, I., Buddery, D., Choi, A., Abma, R., Manning, T., and Pfister, M. [2009] Independent simultaneous sweeping in Libya – full scale implementation and new developments. *79th SEG Annual Meeting*, Expanded Abstracts, **28**, 31-35

Pecholcs, P.I., Lafon, S.K., Al-Ghamdi, T., Al-Shammery, H., Kelamis, P.G., Huo, S.X., Winter, O., Kerboul, J.-B., and Klein, T. [2010] Over 40,000 vibrator points per day with real-time quality control: opportunities and challenges. *80th SEG Annual Meeting*, Expanded Abstracts, **29**, 111-115.

Soubaras, R., 2010, Deghosting by joint deconvolution of a migration and a mirror migration: SEG Technical Program Expanded Abstracts, 29, no. 1, 3406–3410.